

# Association with the Auxiliary Subunit PEX5R/Trip8b Controls Responsiveness of HCN Channels to cAMP and Adrenergic Stimulation

Gerd Zolles,<sup>1</sup> Daniela Wenzel,<sup>2</sup> Wolfgang Bildl,<sup>1</sup> Uwe Schulte,<sup>6</sup> Andreas Hofmann,<sup>3</sup> Catrin S. Müller,<sup>1</sup> Jörg-Oliver Thumfart,<sup>1</sup> Andreas Vlachos,<sup>5</sup> Thomas Deller,<sup>5</sup> Alexander Pfeifer,<sup>3</sup> Bernd K. Fleischmann,<sup>2</sup> Jochen Roeper,<sup>4</sup> Bernd Fakler,<sup>1,7</sup> and Nikolaj Klöcker<sup>1,\*</sup>

<sup>1</sup>Institute of Physiology, University of Freiburg, Engesserstrasse 4, 79108 Freiburg, Germany

<sup>2</sup>Institute of Physiology, Life & Brain Center

<sup>3</sup>Institute of Pharmacology and Toxicology

University of Bonn, Sigmund-Freud-Strasse 25, 53105 Bonn, Germany

<sup>4</sup>Institute of Neurophysiology

<sup>5</sup>Institute of Clinical Neuroanatomy

Neuroscience Center, Goethe-University Frankfurt, Theodor Stern Kai 7, 60590 Frankfurt, Germany

<sup>6</sup>Logopharm GmbH, Engesser Strasse 4, 79108 Freiburg, Germany

<sup>7</sup>Center for Biological Signaling Studies (bioss), Albertstrasse 10, 79104 Freiburg, Germany

\*Correspondence: [nikolaj.kloecker@physiologie.uni-freiburg.de](mailto:nikolaj.kloecker@physiologie.uni-freiburg.de)

DOI 10.1016/j.neuron.2009.05.008

## SUMMARY

Hyperpolarization-activated cyclic nucleotide-gated (HCN) channels are key modulators of neuronal activity by providing the depolarizing cation current  $I_h$  involved in rhythmogenesis, dendritic integration, and synaptic transmission. These tasks critically depend on the availability of HCN channels, which is dynamically regulated by intracellular cAMP; the range of this regulation, however, largely differs among neurons in the mammalian brain. Using affinity purification and high-resolution mass spectrometry, we identify the PEX5R/Trip8b protein as the  $\beta$  subunit of HCN channels in the mammalian brain. Coassembly of PEX5R/Trip8b affects HCN channel gating in a subtype-dependent and mode-specific way: activation of HCN2 and HCN4 by cAMP is largely impaired, while gating by phosphoinositides and basal voltage-dependence remain unaffected. De novo expression of PEX5R/Trip8b in cardiomyocytes abolishes  $\beta$ -adrenergic stimulation of HCN channels. These results demonstrate that PEX5R/Trip8b is an intrinsic auxiliary subunit of brain HCN channels and establish HCN-PEX5R/Trip8b coassembly as a mechanism to control the channels' responsiveness to cyclic nucleotide signaling.

## INTRODUCTION

Hyperpolarization-activated cyclic nucleotide-regulated (HCN) channels are nonselective cation channels assembled as homo- or heterotetramers from the protein subunits encoded by the four members of the HCN channel family (HCN1–4; [Ludwig et al., 1998](#); [Santoro et al., 1998](#)). For activation under physiolog-

ical conditions, HCN channels use a complex gating machinery which is primarily fueled by membrane hyperpolarization and receives strong modulatory input from interactions with cyclic nucleotides (for review, [Robinson and Siegelbaum, 2003](#)) and phosphoinositides such as phosphatidylinositol-4,5-bisphosphate (PIP<sub>2</sub>; [Pian et al., 2006](#); [Zolles et al., 2006](#)). Upon binding to the  $\alpha$  subunit, either modulator allosterically shifts the voltage-dependent activation curve by up to 20 mV toward depolarized potentials and thus increases the number of activatable or activated channels at any given membrane potential in the physiological voltage range.

Once activated, HCN channels give rise to the depolarizing cation current termed  $I_h$  (or  $I_f$ ,  $I_q$ ) that is fundamentally involved in a number of physiological processes. These include the control of pacemaking activity in both heart and brain ([DiFrancesco, 1993](#); [Pape and McCormick, 1989](#)), determination of the resting membrane potential ([Williams and Stuart, 2000](#)), control of membrane resistance and synaptic integration in dendrites ([Magee, 1999](#)) as well as primary sensory transduction ([Stevens et al., 2001](#)).

These functions critically depend on the availability of HCN channels which is determined by their expression on the cell surface and their biophysical properties. Surface expression of HCN channels in brain may be controlled by PEX5R/Trip8b, a HCN interactor that was identified in a yeast-two-hybrid screen and shown to decrease surface half-life of HCN channels in heterologous expression systems ([Santoro et al., 2004](#)). The biophysical availability of HCN channels can be dynamically regulated through the allosteric modulators; in particular, the intracellular concentration of cAMP is known to be effectively regulated on a rapid time scale via different signaling pathways ([Willoughby and Cooper, 2007](#)). Among the most prominent examples of second-messenger controlled HCN functions are the  $\beta$ -adrenergic regulation of heart rate via the control of voltage-dependent HCN gating in sinoatrial node cells ([Brown et al., 1979](#); [DiFrancesco, 1995](#)) and the transition between sleep and wake states of the brain via modulatory control of HCN

channel gating in thalamocortical relay neurons (Pape and McCormick, 1989). In the latter case, activation of ascending reticular brainstem systems leads to increased cAMP levels and thereby mediates a HCN-channel-dependent switch of electrical discharge pattern in thalamocortical relay neurons, which in turn creates an important wake-up signal in the brain. In addition, receptor-mediated regulation of HCN channel activity has been implied in the control of neuronal excitability and information processing in various CNS neurons. This includes modulation of the resting membrane potential of brainstem motoneurons and hippocampal interneurons by norepinephrine, 5-HT, and opioid receptor agonists (Bobker and Williams, 1989; Larkman and Kelly, 1992; Maccaferri and McBain, 1996; Svoboda and Lupica, 1998) as well as the increase in network activity underlying working memory formation by  $\alpha$ 2-adrenergic-triggered inhibition of  $I_h$  via decreasing cAMP levels in prefrontal cortex neurons (Wang et al., 2007).

With respect to the extent of cAMP-induced shifts in voltage-dependent gating of HCN channels, considerable variability ranging from  $\sim$ 2 mV to  $\sim$ 14 mV has been described not only for different cell types (for review, Santoro and Tibbs, 1999) but also in disease states, where reduced cAMP-modulation of HCN channels might, e.g., contribute to epileptogenesis (Kuisle et al., 2006). These differences were attributed to either varying subunit compositions of HCN channels, as distinct HCN subtypes show variable degrees of cAMP-dependent gating (Ishii et al., 1999; Seifert et al., 1999; Chen et al., 2001; Stieber et al., 2005; Zolles et al., 2006) or to posttranslational modification of their gating machinery by protein kinases and phosphatases (Zong et al., 2005; Arinsburg et al., 2006; Huang et al., 2008; Li et al., 2008). Alternatively, HCN channels in the mammalian brain may associate with further yet unknown protein subunits that effectively modulate their gating properties similar to the auxiliary subunits of other ion channel families (Curtis and Catterall, 1984; Isom et al., 1992; Garcia-Calvo et al., 1994; Rettig et al., 1994; Sanguinetti et al., 1996).

By combining affinity-purification of native HCN channel complexes with high-resolution mass spectrometry, we identify PEX5R/Trip8b as the  $\beta$  subunit of HCN channels in the mammalian brain. Association of PEX5R/Trip8b with HCN channels attenuates their modulation by cyclic nucleotides and thus determines their responsiveness to cAMP signaling.

## RESULTS

### Affinity Purification of HCN Channel Complexes

For investigating the molecular entities of HCN channels in the mammalian brain, HCN2-containing channel complexes were affinity purified with a HCN2-specific antibody (anti-HCN2) from membrane fractions that were prepared from total rat brain and efficiently solubilized under conditions preserving high molecular weight complexes (Figures 1A and 2B). Complete eluates of affinity purifications (APs) with anti-HCN2 and several pools of rabbit immunoglobulin G (IgG) serving as negative control were analyzed by high-resolution nanoflow liquid chromatography tandem mass spectrometry (nano-LC MS/MS; Figure 1A). These analyses showed that all four HCN isoforms, HCN1–4, were retained by the anti-HCN2 antibody both specif-

ically and abundantly as indicated by the relative peptide query (rPQ) score and the normalized PQ ( $PQ_{norm}$ ) score, respectively (Table 1). The rPQ-score (ratio of the numbers of MS/MS spectra obtained for a protein in the APs with anti-HCN2 and control IgGs) provides a measure for the purification specificity of a protein (rPQ scores  $>4$  are indicative for specific copurification (Berkefeld et al., 2006)), while the  $PQ_{norm}$  score (number of MS/MS spectra obtained for a given protein divided by the number of theoretically identifiable peptides) estimates its abundance in an AP (Schwenk et al., 2009). The peptides retrieved by mass spectrometry provided coverage of the primary sequence of 57%, 51%, 34%, 31%, for HCN1–4, respectively (Figure 1B). In addition to the HCN  $\alpha$  subunits, MS analysis consistently identified PEX5R (or synonym: Trip8b), a protein previously found as an HCN channel interactor in a yeast two-hybrid screen (Santoro et al., 2004). PEX5R was specifically copurified with high yield (peptides covering 77% of the accessible sequence) under all solubilization conditions used, strongly suggesting that this protein is tightly associated with HCN channels in the CNS (Figure 1C; Table 1).

Coassembly of HCN channels and PEX5R was confirmed by “reverse APs” using a PEX5R-specific antibody (anti-PEX5R) on membrane fractions from rat brain solubilized under the same conditions as before. As illustrated in Figure 2A by the ion chromatogram (intensity of the MS signal over elution time) and the MS/MS spectrum of one selected HCN2-specific peptide (the same as in Figure 1B), the HCN2 protein was specifically copurified with anti-PEX5R (absence of the respective MS signal in IgG controls) at an abundance similar to that seen in APs with the anti-HCN2 antibody (Figure 2A, inset). In addition, HCN-PEX5R coassembly was corroborated by a two-dimensional gel separation of rat brain membrane fractions using blue native polyacrylamide gel electrophoresis (BN-PAGE) and denaturing SDS-PAGE. Subsequent western probing of this separation with anti-HCN2 and anti-PEX5R antibodies revealed close comigration of both proteins indicative for their tight association (Figure 2B). The amounts of HCN and PEX5R proteins in APs with anti-HCN2 and anti-PEX5R were further quantified using the MS signals ( $m/z$  peak volumes) of all HCN and PEX5R peptide fragments obtained in these APs together with a signal calibration determined in nano-LC MS/MS analyses of heterologously expressed PEX5R-HCN fusion proteins (see Experimental Procedures). The results of this quantification showed that the total amount of HCN protein (HCN1–4) was about the same in either AP, strongly suggesting that both HCN and PEX5R proteins are assembled in almost equimolar ratios in the rat brain (Figure 2C).

Moreover, MS analyses of the eluates from anti-PEX5R APs failed to detect other proteins present at an abundance comparable to that of the HCN channel  $\alpha$  subunits (Figure 2D). This result pointed toward a preferred and bimolecular assembly of HCN and PEX5R not requiring further protein partners. The latter was confirmed in an anti-PEX5R AP from *Xenopus* oocytes co-expressing HCN1 and PEX5R; the respective MS analysis retrieved 44 and 25 peptide queries (24 and 19 different peptides) for PEX5R and HCN1, respectively.

In summary, the biochemical analyses showed that HCN channel  $\alpha$  subunits and PEX5R are intimately coassembled

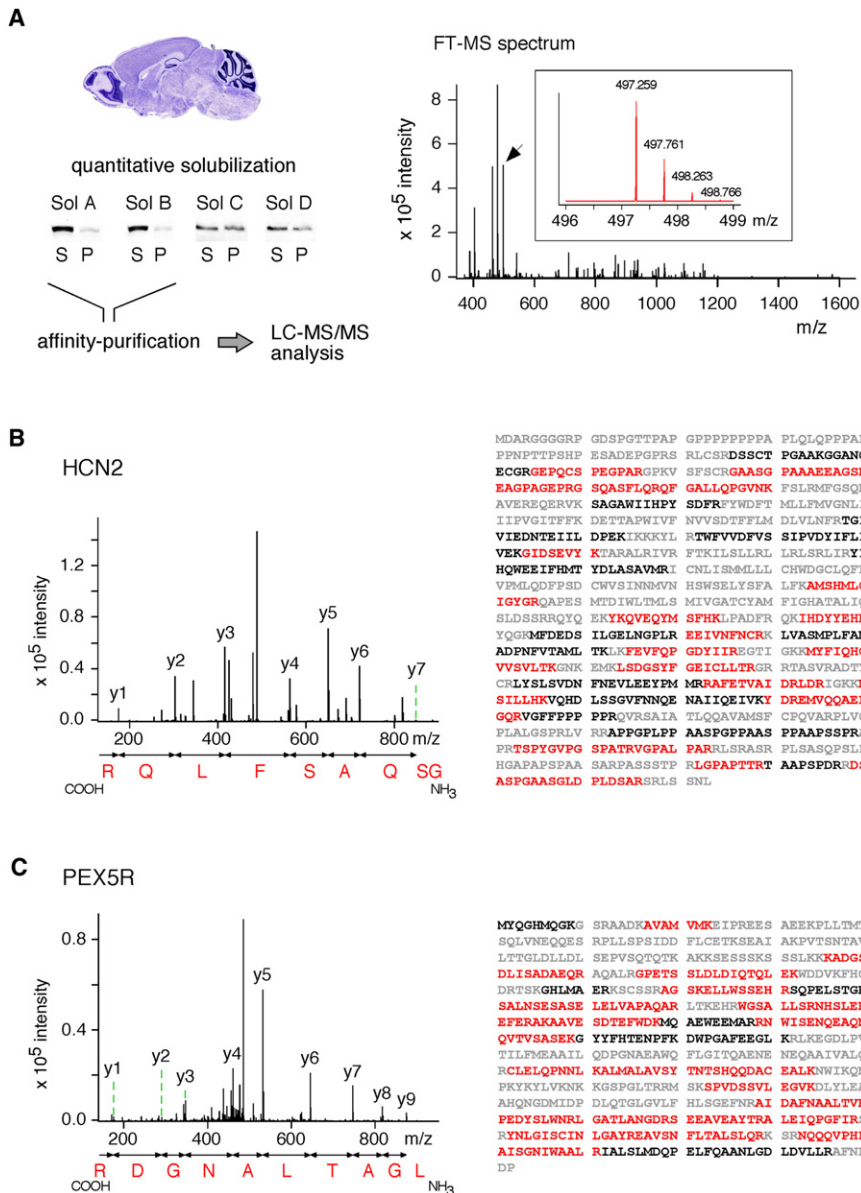


**Figure 1. HCN Channels and PEX5R Are Effectively Copurified from Rat Brain Membrane Preparations**

(A) (Left panel) Scheme of the proteomic approach used for analysis of HCN channel complexes from total rat brain; solubilization conditions A (buffer ComplexioLyte48) and B (buffer ComplexioLyte71) were used in affinity purifications (APs). (Right panel) MS spectrum recorded during high-resolution MS analysis of an eluate from an AP with anti-HCN2. Arrow head denotes a HCN2-specific peptide fragment with a  $m/z$  ratio of 497.259; inset: spectrum of this peptide at enlarged scale indicating the respective isotope peaks.

(B) (Left panel) MS/MS spectrum of the peptide in (A) indicating its amino acid sequence (given in carboxy-to-amino-terminal direction) as derived from its  $y^+$ -ion series. (Right panel) Coverage of the HCN2 primary sequence by the peptides identified with LC-MS/MS. Sequence stretches retrieved by mass spectrometry are in red, those accessible to but not identified are in black, and stretches not accessible to MS/MS analyses are in gray.

(C) MS/MS spectrum of a PEX5R-specific peptide (left panel) retrieved in MS analyses of the same anti-HCN2 AP as in (A) and (B) together with the respective coverage of the PEX5R amino acid sequence (right panel).

in the brain at comparable molar ratios reminiscent of the partnering between voltage-gated cation channels and their auxiliary  $\beta$  subunits.

**PEX5R Antagonizes Activation of HCN Channels by cAMP**

Auxiliary subunits are known to modulate processing and/or the biophysical properties of the pore-forming  $\alpha$  subunits of ion channels (Curtis and Catterall, 1984; Isom et al., 1992; Garcia-Calvo et al., 1994; Rettig et al., 1994; Sanguinetti et al., 1996; An et al., 2000; Estevez et al., 2001). We therefore tested whether coassembly of PEX5R and HCN subunits affects the gating characteristics of the channels in giant inside-out (i-o) patches from *Xenopus* oocytes expressing HCN channels either alone or together with PEX5R. Figure 3A illustrates currents recorded from homo- and heteromeric HCN2 channels in response to hy-

perpolarizing voltage steps and in the presence of a saturating concentration of cAMP (100  $\mu$ M) at the cytoplasmic side. Although both types of channels gave rise to hyperpolarization-activated currents, they differed considerably in their characteristics. While homomeric HCN2 channels provided robust currents at a membrane potential of  $-110$  mV, currents through HCN2 channels coassembled with PEX5R (HCN2 + PEX5R) displayed largely reduced amplitudes under these conditions (Figure 3A, red traces). In addition, PEX5R slowed the time course of channel activation at  $-110$  mV more than 3-fold ( $1.10 \pm 0.19$  s [mean  $\pm$  SD of  $n = 7$  patches] and  $3.75 \pm 0.88$  [n = 6],  $p < 0.0005$ , Student's t test). Further analysis showed that both PEX5R effects, reduction in current amplitude and slowing of the activation time course, resulted from an impaired cAMP gating of the heteromeric HCN2 + PEX5R channels. Thus, PEX5R reduced the cAMP-mediated shift in voltage-dependent activation by about 60% (values for  $\Delta V_{1/2}$  of 7.1 mV and 17.1 mV for HCN2 + PEX5R and HCN2 channels, respectively), without changing the basal voltage-dependence determined in extensively washed-out membrane patches (values for  $V_{1/2}$  of  $-123.2 \pm 3.4$  mV [n = 11] and  $-123.6 \pm 3.1$  mV [n = 15] for HCN2 + PEX5R and HCN2 channels, respectively). Moreover, when corrected for the different cAMP-mediated shifts in voltage-dependence, the activation time constants of homomeric HCN2 and heteromeric

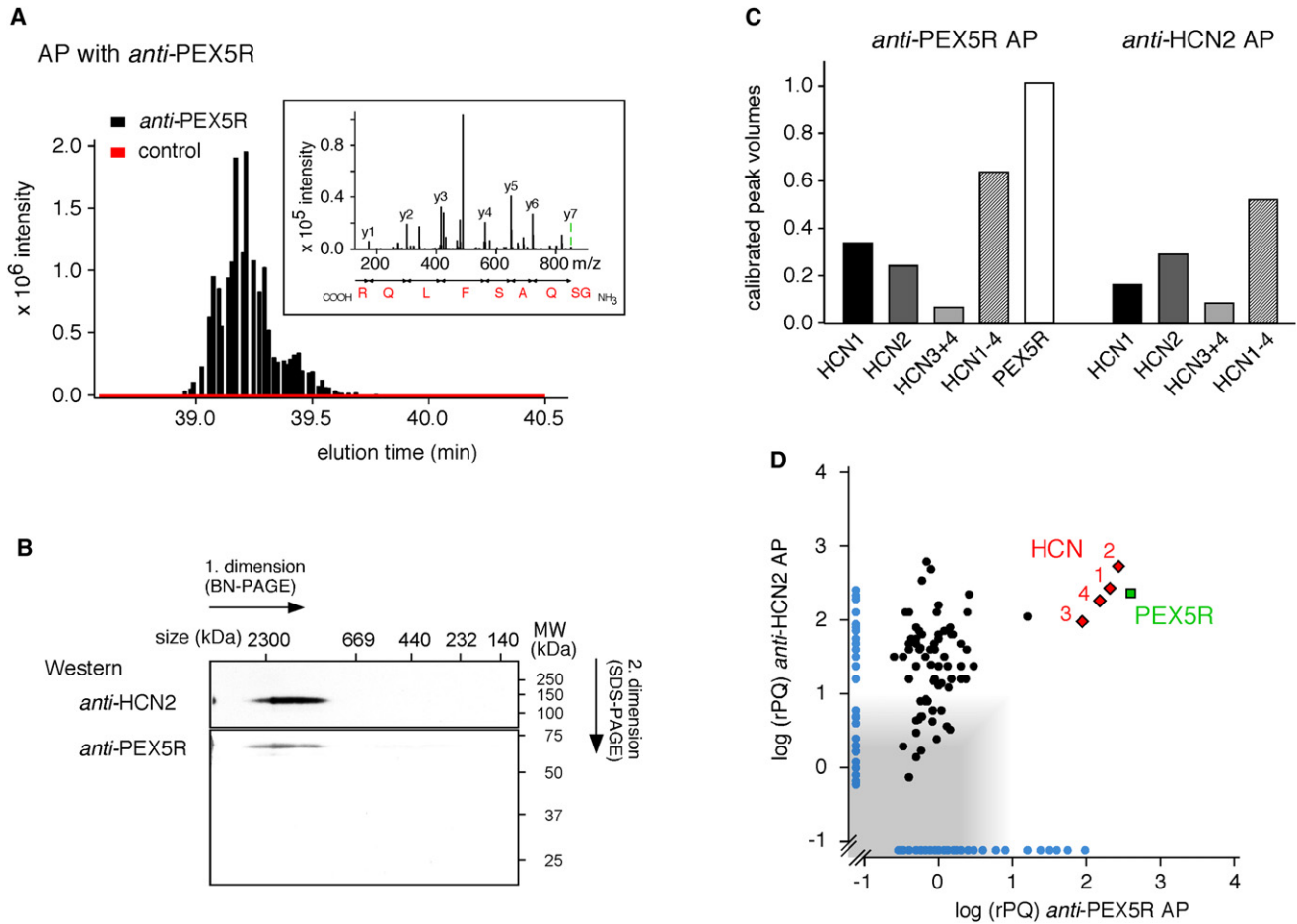


### Figure 2. PEX5R Is Tightly Coassembled with HCN Channels in the Mammalian Brain

(A) Identification of HCN2 in an AP with the *anti*-PEX5R antibody. Ion chromatogram (total ion current) and MS/MS spectrum (inset) of the same HCN2-specific peptide which is shown in Figure 1. The m/z ratio of 497.259 was not detected in APs with preimmunization IgG pools used as a control. Note the similar signal intensities of the HCN2 peptide in APs with both *anti*-HCN2 and *anti*-PEX5R antibodies.

(B) Two-dimensional gel separation of HCN channel complexes in solubilized membrane fractions from total rat brain; the gel separation was western probed with the indicated antibodies. Size (BN-PAGE, derived from standards for high molecular weight complexes) and molecular weight (SDS-PAGE) as indicated.

(C) Bar graph illustrating the abundance of the indicated HCN and PEX5R proteins in APs with *anti*-PEX5R (left) and *anti*-HCN2 (right) antibodies. Quantification of protein amounts used HCN-PEX5R fusion proteins for calibration (see Experimental Procedures); HCN1–4 indicates the sum of all four HCN protein isoforms in the respective AP.

(D) Logarithmic rPQ values of proteins identified in APs with *anti*-HCN2 and *anti*-PEX5R (rPQ values from Table 1). Blue circles refer to proteins identified in only one of the two APs; area shaded in gray highlights nonspecifically purified proteins. Note that only HCN subunits and PEX5R were purified at high abundance in both APs.

HCN2 + PEX5R channels showed no obvious difference (see Figure S1A available online).

The efficacy of the PEX5R-HCN2 interaction was further investigated by titrating the amounts of HCN2 and PEX5R cRNAs injected into oocytes and monitoring the cAMP-induced shift of the steady-state activation curve. As shown in Figure 3C, the cAMP-shift depended on the ratio of the two cRNAs and was minimal at a HCN2/PEX5R cRNA ratio of 1/9. A similar reduction of the cAMP-shift was obtained when PEX5R was fused to the N terminus of the HCN2 protein ( $_{\text{PEX5R}}$ HCN2) ensuring stoichiometric assembly of both proteins into functional HCN channels (Figure 3C). Coexpression of free PEX5R with this fusion construct did not result in a further reduction of the cAMP-shift,

indicating that the PEX5R effect was maximal at a HCN2/PEX5R cRNA ratio of 1/9 (Figure 3C).

Next, we tested the specificity of the gating effect of PEX5R by probing its influence on a cAMP-insensitive mutant of HCN2 (HCN2(R591E)) as well as by probing its interference with the phosphoinositide-mediated modulation of channel gating in HCN2 wild-type. As illustrated in Figure 4, neither voltage-dependent activation of HCN2(R591E) channels was affected by PEX5R (Figure 4A), nor did it influence the modulation of channel activation by phosphoinositides (Figure 4B). Thus, saturating application of PIP<sub>2</sub> onto washed i-o patches resulted in a similar shift in the steady-state activation curve toward more positive potentials in both HCN2 and HCN2 + PEX5R channels

**Table 1. HCN and PEX5R Proteins Affinity Purified with the Indicated Antibodies from Rat Brain Membrane Fractions and Identified by nano-LC MS/MS Analyses (as detailed in Experimental Procedures)**

Protein ID	anti-HCN2 Sol48		anti-HCN2 Sol71		anti-PEX5R Sol71	
	rPQ	PQ <sub>norm</sub>	rPQ	PQ <sub>norm</sub>	rPQ	PQ <sub>norm</sub>
HCN1	468	1.16	262	0.89	200	0.68
HCN2	734	1.86	515	1.81	262	0.92
HCN3	85	0.19	92	0.28	85	0.26
HCN4	277	0.51	177	0.45	298	0.37
PEX5R/Trip8b	253	1.24	223	1.00	443	1.72

rPQ is relative peptide query score; values for rPQ >4 indicate specific copurification of a given protein (Berkefeld et al., 2006). PQ<sub>norm</sub> is normalized peptide query score; the values for PQ<sub>norm</sub> are a quantitative measure for the coverage (and hence the abundance) of a given protein in an AP.

(values for  $\Delta V_{1/2}$  of  $18.0 \pm 0.8$  mV [ $n = 10$ ] and  $17.3 \pm 3.1$  mV [ $n = 12$ ] for HCN2 and HCN2 + PEX5R channels, respectively). Moreover, PEX5R-mediated impairment of cAMP-gating was independent of whether the cyclic nucleotide was applied to washed i-o patches before or after exposure to PIP<sub>2</sub> (Figure 4B).

Together, these results demonstrated that coassembly with PEX5R selectively antagonized the shift in voltage-dependent activation of HCN2 channels by cAMP.

### The Effect of PEX5R on HCN Channel Gating Is Subtype Specific

Next, we investigated the effects of PEX5R on the cAMP-gating of HCN1 and HCN4 channels in i-o patches excised from oocytes that were injected with PEX5R and HCN cRNAs at 1/1 ratios. In HCN4 channels, association with PEX5R antagonized the modulation of channel gating by cAMP very similar in extent to what was observed in HCN2 (values for  $\Delta V_{1/2}$  by cAMP of  $17.6 \pm 1.9$  mV [ $n = 7$ ] and  $10.6 \pm 3.0$  mV [ $n = 12$ ] for HCN4 and HCN4+PEX5R channels respectively,  $p < 0.001$ , Student's t test; Figure 5B). Again, the basal voltage-dependent gating of HCN4 channels, was unaffected by the coassembly with PEX5R (values for  $V_{1/2}$  of  $127.7 \pm 3.8$  mV [ $n = 7$ ] and  $130.8 \pm 4.9$  mV [ $n = 12$ ] for HCN4 and HCN4 + PEX5R channels, respectively,  $p = 0.14$ , Student's t test; Figure 5B).

In contrast to HCN2 and HCN4, PEX5R failed to exert any obvious effect on gating and cAMP modulation of HCN1 channels in excised patches. Thus, the small increase in current amplitude induced by cAMP as a result of an  $\sim 5$  mV shift of the activation curve of HCN1 channels was independent of the coassembly with PEX5R (values for  $V_{1/2}$  of  $98.8 \pm 3.1$  mV [ $n = 28$ ] and  $98.1 \pm 2.3$  mV [ $n = 11$ ] for HCN1 and HCN1 + PEX5R channels, respectively,  $p = 0.7$ , Student's t test; values for  $\Delta V_{1/2}$  by cAMP of  $4.9 \pm 1.2$  mV [ $n = 28$ ] and  $4.5 \pm 1.0$  mV [ $n = 11$ ] for HCN1 and HCN1 + PEX5R channels, respectively,  $p = 0.94$ , Student's t test; Figures 5A and 5B). This lack of effect was not due to low expression or impaired association of PEX5R with HCN1 channels as fusion of both proteins (PEX5R-HCN1) resulted in a similar cAMP-shift of the steady-state activation curve as seen with homomeric HCN1 or heteromeric HCN1 + PEX5R channels (Figure 5B). These results indicated that PEX5R selec-

tively acts on the HCN subtypes where modulation by cAMP is most prominent.

The antagonistic effect of PEX5R on cAMP-gating was recapitulated by lentiviral expression of GFP-fused PEX5R (GFP-PEX5R) in CA1 pyramidal neurons of organotypic hippocampal slice cultures at 6 DIV (Figure 6). At this stage of postnatal development, HCN channels are predominantly composed of HCN2 and HCN4 (Surges et al., 2006), while expression of PEX5R is low or absent (Figure S2). Accordingly, a large cAMP-induced shift in voltage dependent activation of  $I_h$  was observed in mock-infected CA1 pyramidal cells ( $\Delta V_{1/2}$  by cAMP of 19.7 mV as obtained from fits to the mean of 6 neurons), that was markedly reduced upon viral expression of PEX5R ( $\Delta V_{1/2}$  by cAMP of 12.7 mV [ $n = 8$ ];  $p < 0.001$  for the PEX5R-mediated effect, Student's t test; Figures 6A and 6B). As before, basal voltage-dependence of  $I_h$  (determined in the absence of cAMP) was unaffected by expression of GFP-PEX5R (Figure 6B);  $I_h$  amplitudes were slightly reduced (Figure S3).

### The N-Terminal Core of PEX5R Is Necessary for Its Gating Effect

Next, we investigated the molecular determinants of PEX5R involved in its antagonizing effect on cAMP-gating of HCN channels. For this purpose, two N-terminal deletion mutants of PEX5R were constructed, one lacking the very N terminus ( $\Delta 2-41$ ) that is known to be subject to extensive alternative splicing (B. Santoro, personal communication) and another one preserving only the C-terminal half of the protein including the six tetratricopeptide repeats (Figure 7A). As shown in Figure 7B, the deletion mutant PEX5R( $\Delta 2-41$ ) was similarly effective in reducing cAMP modulation of HCN2 channels as PEX5R wild-type, whereas the PEX5R( $\Delta 1-258$ ) mutant failed to affect cAMP-gating of HCN2 channels. This lack of effect could not be attributed to a lack in expression or association with the HCN2 protein, as both PEX5R( $\Delta 1-258$ ) and HCN2 were effectively copurified with the anti-HCN2 antibody (4 and 8 peptide queries, respectively).

These observations implied that the N-terminal core domain of PEX5R was necessary for mediating the gating effect of PEX5R, whereas its C terminus containing the tetratricopeptide repeats was sufficient for biochemical association with HCN2 channels.

### De Novo Expression of PEX5R in Cardiomyocytes Abolishes $\beta$ -Adrenergic Activation of $I_f$

In the mammalian heart, sympathetic stimulation of  $\beta$ -adrenergic receptors in sinoatrial pacemaker cells leads to an acceleration of the heart rate as a result of  $I_f$  activation via an increase in intracellular cAMP levels (DiFrancesco, 1995). This signaling pathway is reconstituted in cultures of dissociated embryonic atrial cardiomyocytes (Reppel et al., 2005). Moreover, as these cells are devoid of endogenous PEX5R (tested by western probing and RT-PCR), de novo expression of PEX5R in these cells by lentiviral gene transfer was used as a model system to explore the significance of the HCN-PEX5R association for HCN channel gating in context of a physiological cAMP signal transduction pathway. As shown in Figure 8A, the  $\beta$ -adrenergic agonist isoprenaline shifted voltage dependent activation of  $I_f$  in mock-infected embryonic atrial cardiomyocytes expressing green fluorescent

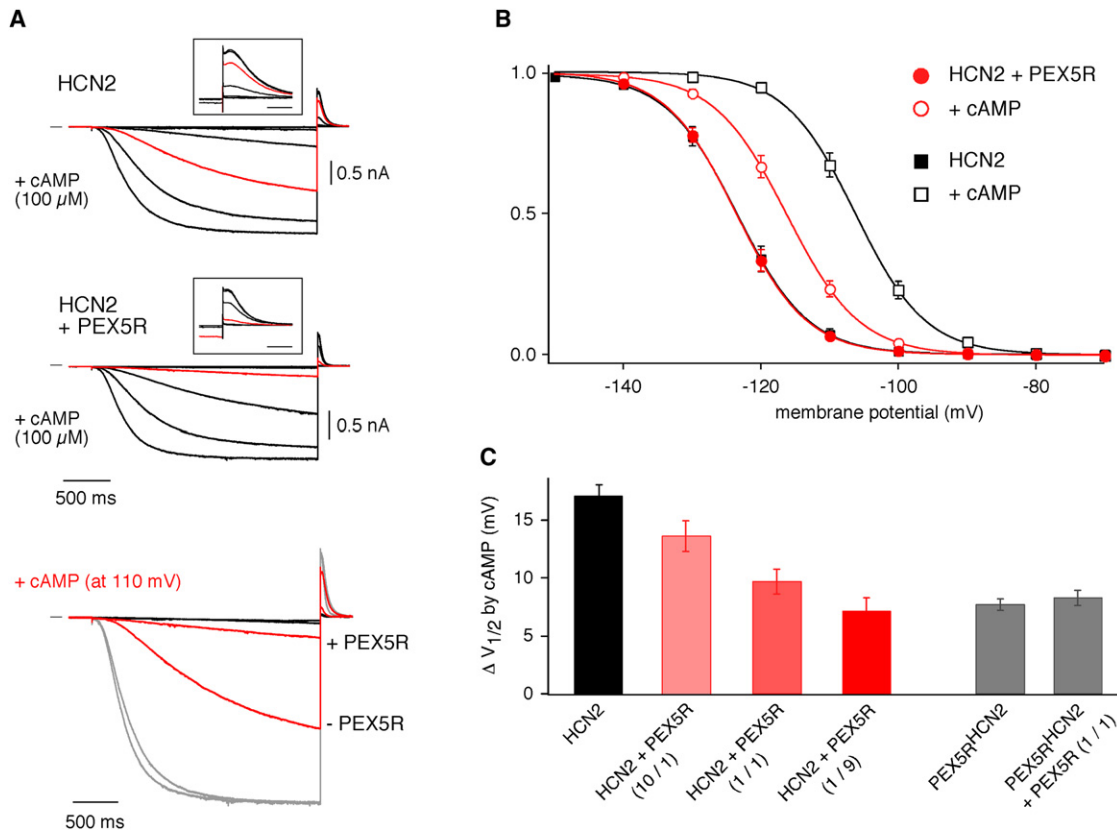


**Figure 3. Coassembly with PEX5R Antagonizes Cyclic Nucleotide Gating of HCN2 Channels**

(A) Representative currents of HCN2 (upper panel) and HCN2 + PEX5R channels (cRNA ratio: 1/9; middle panel) recorded in response to voltage steps to potentials between  $-70$  mV and  $-130$  mV ( $-$ PEX5R) or  $-140$  mV ( $+$ PEX5R) in  $10$  mV increments (holding potential  $0$  mV, tail potential  $50$  mV) in the presence of cAMP ( $100$   $\mu$ M). Traces in red are responses to a step potential of  $-110$  mV. Inset: Tail currents at expanded time scale, bar is  $50$  ms. (Lower panel) Current responses of HCN2 and HCN2+PEX5R channels recorded at  $-110$  mV before (black) and after (red) application of cAMP ( $100$   $\mu$ M). Traces were normalized to maximum current (gray traces). Current and time scales as indicated. Horizontal line is zero current.

(B) Steady-state activation curves of HCN2 channels (black) and HCN2 + PEX5R channels (cRNA ratio: 1/9; red) before (filled symbols) and after application of  $100$   $\mu$ M cAMP (open symbols). Data points are mean ( $\pm$ SEM) of 11–15 patches. Lines are fit of a Boltzmann function to the data with values for  $V_{1/2}$  and slope factor of  $-123.4$  mV ( $5.2$  mV) (HCN2, washed),  $-106.3$  mV ( $5.1$  mV) (HCN2, cAMP),  $-123.6$  mV ( $5.2$  mV) (HCN2 + PEX5R, washed),  $-116.2$  mV ( $5.3$  mV) (HCN2 + PEX5R, cAMP).

(C) Summary of the shifts in activation curve induced by cAMP ( $100$   $\mu$ M) in the indicated channels (see text). Data points are mean ( $\pm$ SD) of 6–23 patches.

protein (GFP) by  $5.3 \pm 0.5$  mV (mean  $\pm$  SEM of 15 cells). Expression of PEX5R C terminally fused to GFP ( $GFP$ -PEX5R), however, completely prevented the isoprenaline-induced shift in voltage dependent activation of  $I_h$  in these cells ( $\Delta V_{1/2}$  by isoprenaline of  $-0.3 \pm 0.7$  mV [ $n = 9$ ];  $p < 0.001$  for the PEX5R mediated effect, Student's  $t$  test; Figure 8B). Functional integrity of the fusion protein was tested in excised patches from *Xenopus* oocytes (data not shown).

These results from cardiomyocytes demonstrated that coassembly with PEX5R limits the response sensitivity of HCN channels to physiological cyclic nucleotide signaling conditions.

## DISCUSSION

The central finding of this study is the identification of PEX5R as the predominant auxiliary subunit of HCN channels in the

mammalian brain. Coassembly with PEX5R specifically antagonizes modulation of HCN channel gating by cAMP, thus providing a potent mechanism to control the responsiveness of  $I_h$  to cyclic nucleotide signaling.

## Molecular Composition of HCN Channels in the Mammalian Brain

The molecular composition of HCN channels in the rat brain was investigated using a comprehensive approach with native PAGE analysis, APs combined with LC-MS/MS analysis and heterologous expression of protein complexes (Berkefeld et al., 2006; Schulte et al., 2006; Schwenk et al., 2009). HCN2 containing channel complexes were almost completely solubilized and exhibited high apparent molecular weight in native gels (approximately  $0.8$ – $2$  MDa; Figure 2B) demonstrating that most HCN channels are not just tetramers of  $\alpha$  subunits (expected

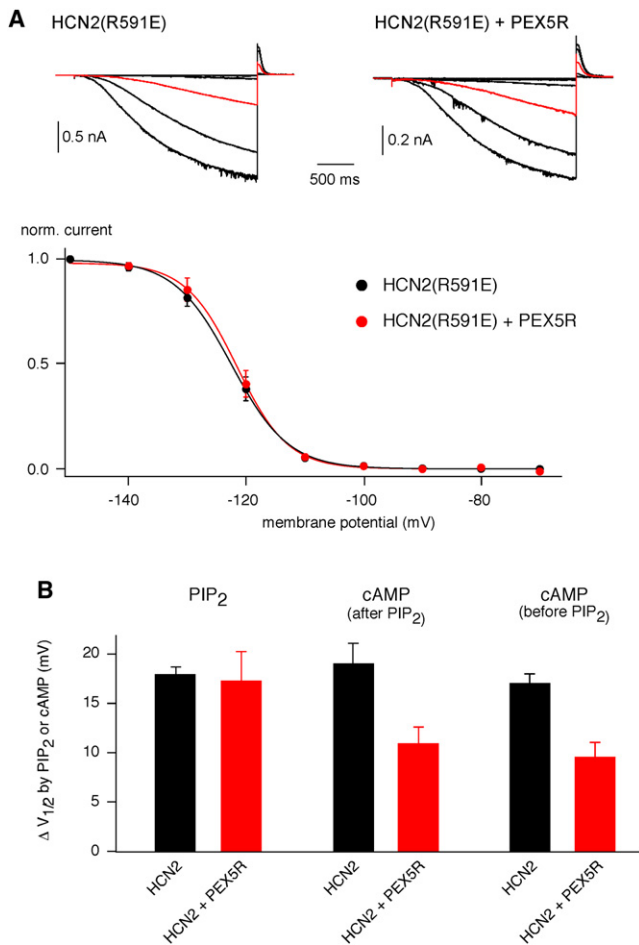


**Figure 4. The Effect of PEX5R on HCN Channel Gating Is Mode Specific**

(A) Representative currents of HCN2(R591E) mutant channels and HCN2(R591E) + PEX5R channels (cRNA ratio: 1/1; upper panel) recorded in response to voltage steps to potentials between  $-70$  mV and  $-140$  mV in  $10$  mV increments (holding potential  $0$  mV, tail potential  $50$  mV). Traces in red are responses to a step potential of  $-120$  mV. Current and time scales as indicated. Lower panel, steady-state activation curves of HCN2(R591E) mutant channels (black) and HCN2(R591E)+PEX5R channels (cRNA ratio: 1/1; red). Data points are mean ( $\pm$ SEM) of 5 patches. Lines are fit of a Boltzmann function to the data with values for  $V_{1/2}$  and slope factor of  $-122.5$  mV ( $4.8$  mV) (HCN2(R591E)),  $-121.6$  mV ( $4.4$  mV) (HCN2(R591E) + PEX5R). (B) Summary of the shifts in activation curve of HCN2 and HCN2 + PEX5R channels (cRNA ratio: 1/1) induced by PIP<sub>2</sub> ( $10$   $\mu$ M) or by cAMP ( $100$   $\mu$ M) before and after application of PIP<sub>2</sub>. Data points are mean ( $\pm$ SD) of 10–12 patches.

molecular weight of  $\sim 0.5$  MDa) but are rather associated with further protein partners. In fact, besides HCN isoforms 1–4, APs of HCN2 channels efficiently retrieved PEX5R, a protein previously reported as an HCN2 interactor in a yeast-two-hybrid screen (Santoro et al., 2004). Quantitative evaluation of MS data using peptide peak intensities and calibration with fusion proteins showed that HCN and PEX5R proteins were copurified in comparable molar amounts (Figure 2C). Moreover, relative participation (molar ratios) of the four HCN subunits found in

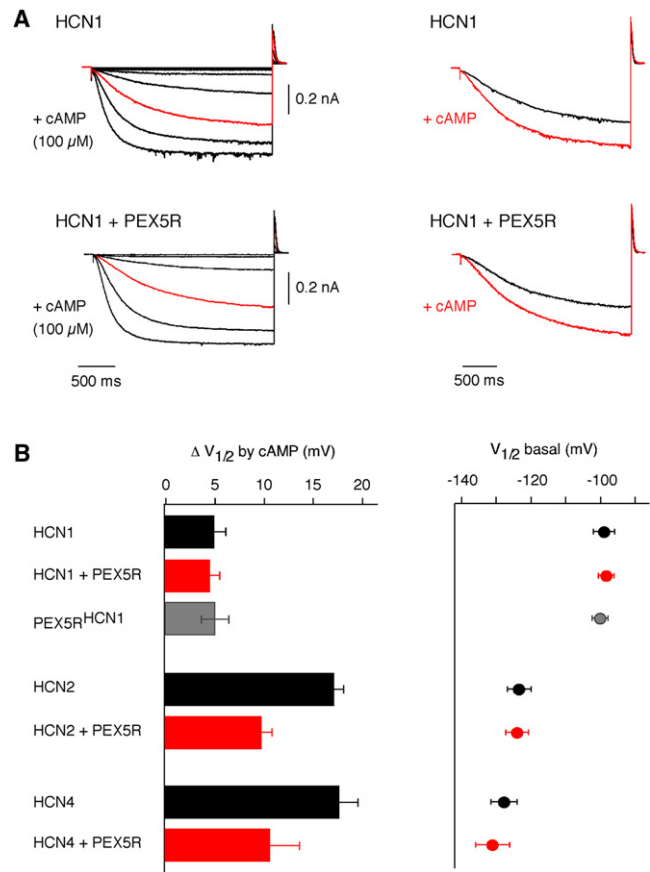
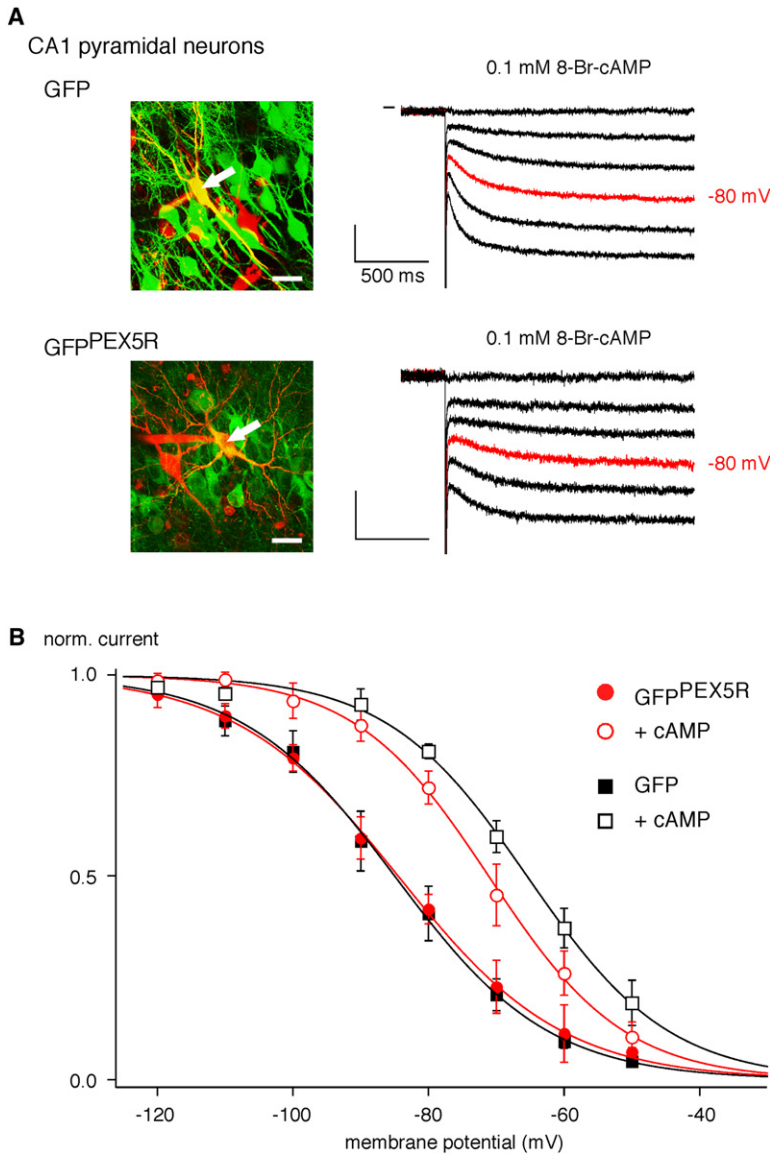


**Figure 5. The Effect of PEX5R on HCN Gating Is Subtype Specific**

(A) Representative currents of HCN1 and HCN1 + PEX5R channels (cRNA ratio: 1/1; upper and lower, left) recorded in response to voltage steps to potentials between  $-50$  mV and  $-120$  mV in  $10$  mV increments (holding potential  $0$  mV, tail potential  $50$  mV) in the presence of  $100$   $\mu$ M cAMP. Traces in red are responses to a step potential of  $-100$  mV. Representative currents of HCN1 and HCN1 + PEX5R channels (upper and lower, right) recorded at  $-100$  mV before (black) and after (red) application of  $100$   $\mu$ M cAMP. Current and time scales as indicated. (B) Summary of the cAMP-induced shifts in activation curve and  $V_{1/2}$  of basal voltage dependence of the indicated channels (see text). Data points are mean ( $\pm$ SD) of 7–28 patches.

APs with anti-PEX5R and anti-HCN2 was very similar and in reasonable agreement with published data on both mRNA and protein expression of HCN isoforms in the CNS (Monteggia et al., 2000; Notomi and Shigemoto, 2004). The comigration of PEX5R and HCN2 in the two-dimensional gel separation (Figure 2B) corroborated their tight association independent of our APs. Assembly of HCN and PEX5R occurs through direct protein-protein interactions as both proteins were effectively copurified from oocytes coexpressing HCN1 or HCN2 and PEX5R.

Thus, our biochemical and proteomic data establish PEX5R as the predominant  $\beta$  subunit coassembled with the vast majority of HCN channels in the mammalian brain. However, our data do not rule out populations of HCN channels in the CNS that lack PEX5R or that associate with other proteins nor do they



elucidate the stoichiometry of HCN to PEX5R subunits in HCN channel complexes.

### Significance of HCN-PEX5R Association for Channel Gating

Cyclic nucleotides increase the number of activatable or activated channels at any given membrane potential in the physiological voltage range by shifting their voltage-dependent activation curve to more depolarized membrane potentials (DiFrancesco and Tortora, 1991). Upon binding to the cyclic nucleotide binding domain (CNBD), they are thought to relieve inhibition of the channel imposed by the concerted action of the CNBD and the C-linker connecting the CNBD to the transmembrane core domain of the channels (Wainger et al., 2001; Wang et al., 2001).

Our *i-o* patch recordings on HCN-PEX5R complexes showed that the auxiliary PEX5R subunit selectively antagonizes the

### Figure 6. Expression of PEX5R Impairs Cyclic Nucleotide Gating of HCN Channels in Hippocampal CA1 Pyramidal Cells

(A) (Left panel) Confocal images of the CA1 region of organotypic slice cultures 4 days following transduction with lentivirus driving expression of either GFP (upper panel) or GFPPEX5R (lower panel). GFP-negative (red) and GFP-positive CA1 neurons (yellow; arrows) were patched with pipettes containing a red fluorescent dye (Alexa 566). (Right panel) HCN-mediated currents recorded from CA1 pyramidal neurons expressing GFP (upper panel) or GFPPEX5R (lower panel) in response to 2 s hyperpolarizing voltage steps from a holding potential of  $-50$  mV (increments of 10 mV). Cells were dialyzed with pipette solutions containing 0.1 mM 8-Br-cAMP; current responses to  $-80$  mV are shown in red. Scale bars are 50 pA and 500 ms.

(B) Steady-state current-voltage relation of HCN currents recorded from CA1 neurons expressing either GFP (black symbols) or GFPPEX5R (red symbols) in experiments as in (A) without and with 0.1 mM 8-Br-cAMP in the patch pipette. Data points are mean  $\pm$  SEM of 6–8 neurons. Continuous lines are fit of a Boltzmann function to the data with values for  $V_{1/2}$  and slope factor of  $-84.3$  mV (12.0 mV) (GFPPEX5R, washed)  $-71.6$  mV (10.1 mV) (GFPPEX5R, +cAMP),  $-84.8$  mV (11.2 mV) (GFP, washed),  $-65.1$  mV (10.4 mV) (GFP, +cAMP).

disinhibition by cAMP in HCN2 and HCN4 channels without any detectable effect on the modulatory action of the phosphoinositide PIP<sub>2</sub> or on the basal voltage-dependence of the channels' gating machinery (Figures 3 and 4). Similar results were obtained in a neuronal cell context upon expression of PEX5R in CA1 pyramidal cells in organotypic hippocampal slice cultures (Figure 6). Mechanistically, the cAMP-antagonizing effect of PEX5R most likely results from interference with the allosteric coupling between CNBD and channel core as binding of cAMP to the CNBD was not influenced by the coassembled PEX5R (Figure S1B). Yet the exact molecular determinants of this allosteric interference as well as the interaction interface between the PEX5R and the HCN proteins

remain to be identified. At this point, deletion analysis revealed that the C terminus of PEX5R harboring the tetratricopeptide repeats is sufficient for biochemical interaction with HCN channels, while its N-terminal core region is required for antagonizing cAMP-gating. As only the very N terminus of PEX5R but not the N-terminal core is subject to alternative splicing (Santoro et al., 2009, this issue of *Neuron*), the effect on cAMP-gating should be preserved in all PEX5R isoforms.

The extent of the cAMP-antagonizing effect of PEX5R may be determined by the stoichiometry of the PEX5R-HCN interaction as inferred from the titration experiment in Figure 3C or by further yet unknown mechanisms including posttranslational modifications. In any case, PEX5R failed to fully abolish cAMP-modulation even when overexpressed or directly fused to the HCN  $\alpha$  subunit (Figure 3C), thus converting HCN2 and 4 into HCN1-like channels with a residual cAMP-shift of their voltage-dependent activation (Chen et al., 2001; Wang et al., 2001).

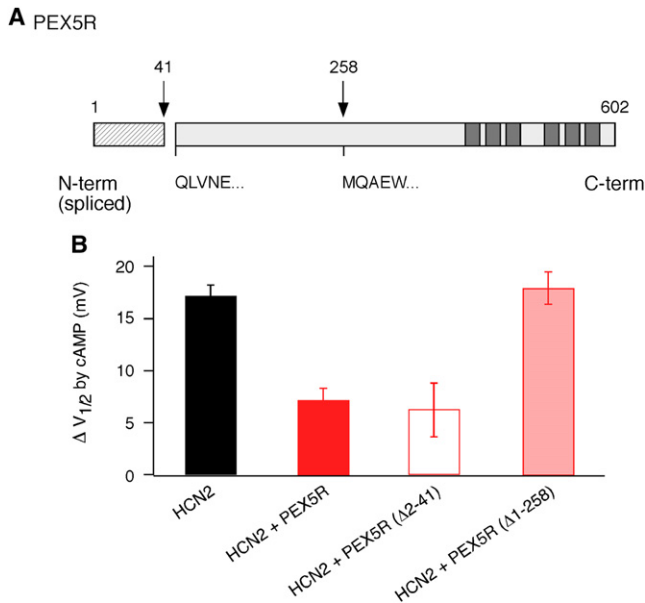


**Figure 7. The N-Terminal Core Is Responsible for the Gating Effect of PEX5R**

(A) Schematic drawing of PEX5R. Numbers and letters referring to the amino acid sequence of PEX5R (SwissProt accession number: Q925N3) indicate the deletion constructs used; dark gray bars represent the six tetratricopeptide repeats in the C terminus of the protein.

(B) Summary of the cAMP-induced shifts in activation curve determined for the indicated wild-type and mutant channels (HCN2 to PEX5R wt/mutant cRNA ratio: 1/9; data points are mean ( $\pm$ SD) of 5–15 patches.

**Significance of HCN-PEX5R Association for Responsiveness of HCN Channels to Cyclic Nucleotide Gating**

The PEX5R-mediated impairment of cAMP modulation of HCN channels would be expected to reduce recruitment of  $I_h$  by cyclic nucleotides. We probed this prediction in the cellular context of embryonic cardiomyocytes where cAMP signaling through  $\beta$ -adrenergic receptors is well established (Ji et al., 1999; Reppel et al., 2005). In fact, whole-cell recordings from these cells demonstrated that  $\beta$ -adrenergic stimulation increases  $I_f$  amplitudes in the physiologically relevant voltage-range by shifting the activation curve of the HCN channels by  $\sim 5$  mV (Figure 7A). This shift in activation was abolished upon de novo expression of PEX5R (Figure 7B) emphasizing that assembly with the PEX5R subunit is sufficient to suppress receptor-mediated stimulation of  $I_f$ . This result together with the data from functional proteomics imply that PEX5R may act as a determinant controlling responsiveness of neuronal HCN channels to receptor-mediated cyclic nucleotide signaling.

**EXPERIMENTAL PROCEDURES**

**Molecular Biology**

In vitro transcription and injection of cRNA into *Xenopus* oocytes was done as described (Fakler et al., 1995). GenBank accession numbers of the cDNAs used were AJ225123.1 (HCN1), AJ225122.1 (HCN2), AJ132429.1 (HCN4), NM\_173152 (PEX5R/Trip8b). Site-directed mutagenesis was performed as described before (Hardel et al., 2008). All cDNAs were verified by sequencing.

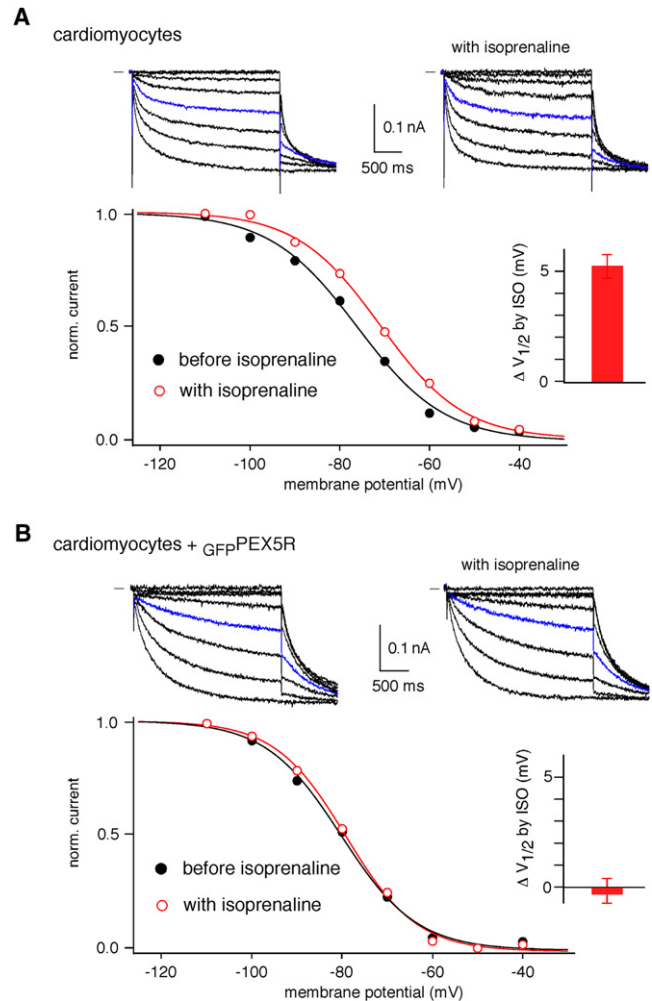


**Figure 8. De Novo Expression of PEX5R in Embryonic Cardiomyocytes Abolishes  $\beta$ -Adrenergic Activation of  $I_f$**

(A) Representative HCN channel-mediated currents ( $I_f$ ) recorded in atrial embryonic cardiomyocytes under control conditions (upper, left) and during adrenergic stimulation with isoprenaline (100 nM; upper right). Currents were recorded in response to voltage steps to potentials between  $-40$  mV and  $-110$  in 10 mV increments (holding potential  $-40$  mV, tail potential  $-110$  mV). Traces in blue are responses to a step potential of  $-80$  mV. Current and time scales as indicated. Lower panel, steady-state activation curves of  $I_f$  determined from the experiments above. Lines are fit of a Boltzmann function to the data with values for  $V_{1/2}$  and slope factor of  $-76.1$  mV and  $9.7$  mV (control), and  $-70.9$  mV and  $9.3$  mV (stimulated). Inset, summary of the shifts in activation curve of  $I_f$  induced by isoprenaline. Data are mean ( $\pm$ SEM) of 15 cardiomyocytes.

(B) Experiments as in (A) performed in cardiomyocytes expressing GFP-PEX5R. Inset, Data are mean ( $\pm$ SEM) of 9 cardiomyocytes.

**Biochemistry**

**Preparation of Membrane Solubilisates**

Synaptosomal-enriched protein fractions were prepared from freshly isolated adult rat brains (Wistar,  $\geq$  P30) by isotonic homogenization and hypotonic lysis of dense vesicles followed by separation on a sucrose step gradient (interface consisting primarily of synaptosomal membrane vesicles; Feigenbaum et al., 1988; Knaus et al., 1995). Solubilization of membrane protein complexes was achieved by suspension of vesicles in ComplexioLyte buffers 48 and 71 (LOGO PHARM GmbH, Germany; 1 mg protein/ml, with protease inhibitors added) at

4°C for 30 min followed by ultracentrifugation (15 min at 130,000  $\times$  g). For the preparation of PEX5R-HCN1 and PEX5R-HCN2 fusion proteins as quantification standards (Beynon et al., 2005), *Xenopus* oocytes injected with the respective cRNAs (cultivated for 4 days) were used as source material.

#### Affinity Purification (AP)

Brain membrane solubilisates (10 ml) were incubated for 2 hr at 4°C with 50  $\mu$ g immobilized affinity-purified rabbit anti-HCN2 (APC-030, Alomone Labs, Israel), rabbit anti-PEX5R (kind gift of B. Santoro), or control IgG pools (Upstate). After washing (3  $\times$  5 min), bound proteins were eluted with Laemmli buffer (DTT added after elution). Fusion protein constructs were purified from oocyte membrane solubilisates (ComplexioLyte 71) using 5  $\mu$ g immobilized anti-PEX5R and anti-HCN2, respectively. Prior to tryptic digestion, all eluates were shortly run on SDS-PAGE gels and silver stained.

#### Native Gel Electrophoresis

Solubilized (salt replaced by 1 M betaine) protein complexes were supplied with Coomassie G250 (0.025% final concentration) and resolved on a 2–15% linear native polyacrylamide gel (BNPage; Schagger et al., 1994). A mixture of native proteins (GE Healthcare) was run as complex size standard in the first dimension. For denaturing separation in the second dimension, gel lanes were excised, equilibrated in Laemmli buffer, and run on a 8% SDS-PAGE gel. After electroblotting on PVDF membrane, western analysis was performed with anti-HCN2 visualized by anti-rabbit IgG-HRP (Santa Cruz Biotechnologies) and developed with ECL Plus (GE Healthcare).

#### Mass Spectrometry

Protein samples were in-gel digested with trypsin as described previously (Pandey et al., 2000). Extracted peptides were redissolved in 0.5% trifluoroacetic acid and loaded on a C18 PepMap100 precolumn (5  $\mu$ m; Dionex) using an UltiMate 3000 HPLC (Dionex). Peptides were then eluted with an aqueous-organic gradient, resolved on a 75  $\mu$ m column (PicoTip Emitter; tip: 8  $\pm$  1  $\mu$ m; New Objective) packed with ReproSil-Pur 120 ODS-3 (C18; 3  $\mu$ m; Dr. A. Maisch, Ammerbuch-Entringen, Germany) and directly electrosprayed into an LTQ-FT mass spectrometer (Thermo Scientific; ion source: Proxeon). Each scan cycle consisted of one FTMS full scan and up to five ITMS dependent MS/MS scans of the five most intense ions. Dynamic exclusion (30 s, mass width 20 ppm) and monoisotopic precursor selection were enabled. Extracted MS/MS spectra were searched against the Swissprot database (Mammalia) using the Mascot search engine (Matrix Science) accepting common variable modifications and one missed tryptic cleavage. Peptide tolerance was  $\pm$  10 ppm and MS/MS tolerance was  $\pm$  0.8 Da. Peptide peak volumes (integral of  $m/z$  signals, also termed extracted ion current, XIC) were determined and aligned with respect to their retention times using MsInspect (Computational Proteomics Laboratory, Fred Hutchinson Cancer Research Center, Seattle, WA).

MS results were evaluated as follows: The relative peptide query (rPQ) score was calculated as a measure of the purification specificity of proteins identified in a given AP; rPQ scores  $>$ 4 are indicative for specific copurification (Berkefeld et al., 2006). To estimate abundance of a given protein, the number of queries (sum of all MS/MS spectra) was divided by the number of peptides theoretically identifiable by mass spectrometry (6–25 amino acids in length) for the respective protein (normalized PQ score,  $PQ_{norm}$ ). More accurate quantification was achieved by evaluating the XIC values that are directly proportional to the abundance of the respective peptide (Figure 2B). The XICs of peptides consistently identified and specific for each protein were summed up and divided by the sum of XICs of the corresponding peptides obtained from LC-MS/MS analysis of the purified fusion constructs PEX5R-HCN1 and PEX5R-HCN2 serving as a standard. Using the XICs of the fused PEX5R as a common reference, molar ratios of PEX5R, HCN1, and HCN2 were obtained. The fraction of HCN isoforms 3 and 4 in the respective APs was calculated as the difference between XICs of all subtype-specific HCN1–4 peptides and the XICs of HCN1- and HCN2-specific peptides divided by the XICs of HCN1- and HCN2-specific peptides identified with the purified standard fusion constructs (Beynon et al., 2005).

#### Electrophysiology and Data Analysis of Recombinant HCN Channels

Electrophysiological recordings from giant inside-out patches excised from oocytes were performed at room temperature (22°C–24°C) as described

previously (Zolles et al., 2006). Currents were recorded with an EPC9 amplifier, low-pass filtered at 1 kHz, and sampled at 2 kHz; capacitive transients were compensated with the automated circuit of the EPC9. Pipettes made from thick walled borosilicate glass had resistances of 0.3–0.6 M $\Omega$  when filled with (in mM): 120 KCl, 10 HEPES, and 1.0 CaCl<sub>2</sub> (pH adjusted to 7.2). Intracellular solution ( $K_{int}$ ) applied via a gravity-driven multibarrel pipette was composed as follows (mM): 100 KCl, 10 K<sub>2</sub>EGTA, 10 HEPES (pH 7.2). All substances were dissolved and diluted to their final concentration in intracellular solution. L- $\alpha$ -Phosphatidyl-D-myo-inositol-4,5-bisphosphate (PIP<sub>2</sub>, Roche Molecular Diagnostics or Avanti Polar Lipids) was suspended in intracellular solution at a concentration of 1 mM, sonicated for 10 min in a cold water bath, aliquoted, and stored at –20°C. Samples were thawed on the day of use, sonicated for another 10 min, and diluted to their final concentration of 10  $\mu$ M with intracellular solution.

Steady-state activation curves were determined with a tail-current protocol. Briefly, preconditioning voltage steps (from a holding potential of 0 mV) were applied to potentials between –50 mV and –150 mV for durations ranging between 1.5 s and 5 s, before the membrane potential was stepped to 50 mV for 500 ms to elicit HCN tail currents. Currents recorded at the tail potential were normalized to maximum, plotted versus the preconditioning potential, and fitted with a Boltzmann function (see above). Curve fitting and further data analysis were done with Igor Pro 4.05A on a Macintosh G4. Data are given as mean  $\pm$  SD, unless otherwise stated.

#### Preparation of Lentiviral Vectors

The HIV-derived lentiviral vector (CMV-GFP) was previously described (Pfeifer et al., 2001). CMV-GFP-PEX5R was generated by replacing the eGFP cDNA with the coding sequence for the GFP-PEX5R fusion protein. High-titer lentivector preparations were produced as previously described (Pfeifer et al., 2002). In brief, lentivector and packaging plasmids were transfected into HEK293T cells. Lentiviral particles were pseudotyped with the G glycoprotein of the vesicular stomatitis virus. Virus was harvested 48 and 72 hr after transfection, concentrated by ultracentrifugation and resuspended in HBSS (Hanks' Balanced Salt Solution).

#### Recordings from Early Embryonic Cardiomyocytes

Murine embryonic atria (E11.5) were harvested from CD1 mice, enzymatically isolated and plated on gelatine-coated coverslips (Fleischmann et al., 2004). The cells were infected with the lentiviral vectors CMV-GFP (control) or CMV-GFP-Trip8b/PEX5R in a volume of 300  $\mu$ l. The transduced cells displayed EGFP expression 2 days after transduction. For electrophysiological recordings, the coverslips were placed into a recording chamber, transduced cells were identified using a fluorescence microscope, and patch-clamp experiments performed in the whole-cell configuration as previously reported (Fleischmann et al., 2004; Zolles et al., 2006). For most experiments, infection with the two different constructs and electrophysiological measurements were performed in parallel. The following solutions were used (in mM): extracellular solution—140 NaCl, 5.4 KCl, 2.0 MgCl<sub>2</sub>, 1.8 CaCl<sub>2</sub>, 10 HEPES, 1 BaCl<sub>2</sub>, 2 4-aminopyridine, 10 glucose (pH 7.4); intracellular solution—12 NaCl, 10 HEPES, 2 MgATP, 10 EGTA, 0.1 NaGTP, 130 K-aspartate (pH 7.2).

Data were sampled at 3 kHz and filtered with 0.5 kHz. Steady-state activation curves were determined using a 2 step I-V protocol: hyperpolarizing voltage steps (2.5 s) were applied from –40 to –110 mV (10 mV increments) from a holding potential of –40 mV, followed by a hyperpolarizing voltage step (2.5 s) to –110 mV (frequency 0.1 Hz; Zolles et al., 2006). Available  $I_f$  was determined by subtracting the current amplitude at the beginning of the second voltage step from the mean current at the end of the step.  $V_{1/2}$  and slope values were obtained from fits of a Boltzmann function to the data described above. Current amplitudes (step from –40 mV to –110 mV) did not significantly differ in control and CMV-GFP-Trip8b/PEX5R transduced cells.

Isoprenaline (ISO) and 3-isobutyl-1-methylxanthine (IBMX, Sigma, Germany) are known to strongly stimulate early embryonic cardiomyocytes (Ji et al., 1999) and a final concentration of 100 nM ISO and 100  $\mu$ M IBMX were used to strongly stimulate  $I_f$ . For analysis, exclusively cells with stable  $R_s$  values  $<$ 15 M $\Omega$  during the experiment were used.

### Recordings from Organotypic Hippocampal Slice Cultures

Organotypic hippocampal slice cultures were prepared from mouse brain as previously described (Del Turco and Deller, 2007). GFP and GFP-PEX5R lentiviral expression constructs were applied on the second day in vitro (2DIV) and transduced GFP-positive CA1 neurons were studied at room temperature using the whole-cell patch-clamp configuration as described (Lammel et al., 2008). K-gluconate pipette solutions without or with 0.1 mM 8-Br-cAMP were dialyzed in the whole-cell configuration ( $R_s < 10 \text{ M}\Omega$ ) for at least 5 min before  $I_h$ -currents were elicited in the voltage-clamp mode. Hyperpolarizing voltage steps (2 s) were applied from  $-50$  to  $-120$  mV (10 mV increments) from a holding potential of  $-50$  mV, followed by a hyperpolarizing voltage step (0.5 s) to  $-100$  mV or  $-120$  mV. Conductance-voltage (g-V) relationships were constructed based on tail current amplitudes and fitted with Boltzmann functions to determine the values for  $V_{1/2}$  and slopes of  $I_h$  currents in CA1 neurons expressing GFP or GFP-PEX5R. Mean normalized g-V relationships were constructed by averaging individual normalized g-V data of  $n = 4-8$  CA1 neurons and fitted with a Boltzmann function.

### SUPPLEMENTAL DATA

Supplemental Data include three figures and can be found with this article online at [http://www.cell.com/neuron/supplemental/S0896-6273\(09\)00359-6](http://www.cell.com/neuron/supplemental/S0896-6273(09)00359-6).

### ACKNOWLEDGMENTS

We thank Dr. B. Santoro for the gift of the anti-Trip8b/PEX5R antibody and A. Haupt for bioinformatics support. The work was funded by grants of the Deutsche Forschungsgemeinschaft (DFG) to B.F. (GRK 843, EXC 294 (bloss)) and to N.K. (KL1168/6).

Accepted: May 7, 2009

Published: June 24, 2009

### REFERENCES

- An, W.F., Bowlby, M.R., Betty, M., Cao, J., Ling, H.P., Mendoza, G., Hinson, J.W., Mattsson, K.I., Strassle, B.W., Trimmer, J.S., and Rhodes, K.J. (2000). Modulation of A-type potassium channels by a family of calcium sensors. *Nature* 403, 553–556.
- Arinsburg, S.S., Cohen, I.S., and Yu, H.G. (2006). Constitutively active Src tyrosine kinase changes gating of HCN4 channels through direct binding to the channel proteins. *J. Cardiovasc. Pharmacol.* 47, 578–586.
- Berkefeld, H., Sailer, C.A., Bildl, W., Rohde, V., Thumfart, J.O., Eble, S., Klugbauer, N., Reisinger, E., Bischofberger, J., Oliver, D., et al. (2006). BKCa-Cav channel complexes mediate rapid and localized Ca<sup>2+</sup>-activated K<sup>+</sup> signaling. *Science* 314, 615–620.
- Beynon, R.J., Doherty, M.K., Pratt, J.M., and Gaskell, S.J. (2005). Multiplexed absolute quantification in proteomics using artificial QCAT proteins of concatenated signature peptides. *Nat. Methods* 2, 587–589.
- Bobker, D.H., and Williams, J.T. (1989). Serotonin augments the cationic current  $I_h$  in central neurons. *Neuron* 2, 1535–1540.
- Brown, H.F., DiFrancesco, D., and Noble, S.J. (1979). How does adrenaline accelerate the heart? *Nature* 280, 235–236.
- Chen, S., Wang, C., and Siegelbaum, S.A. (2001). Properties of hyperpolarization-activated pacemaker current defined by coassembly of HCN1 and HCN2 subunits and basal modulation by cyclic nucleotide. *J. Gen. Physiol.* 117, 491–504.
- Curtis, B.M., and Catterall, W.A. (1984). Purification of the calcium-antagonist receptor of the voltage-sensitive calcium-channel from skeletal-muscle transverse tubules. *Biochemistry* 23, 2113–2118.
- Del Turco, D., and Deller, T. (2007). Organotypic entorhino-hippocampal slice cultures – a tool to study the molecular and cellular regulation of axonal regeneration and collateral sprouting in vitro. *Methods Mol. Biol.* 399, 55–66.
- DiFrancesco, D. (1993). Pacemaker mechanisms in cardiac tissue. *Annu. Rev. Physiol.* 55, 455–472.
- DiFrancesco, D. (1995). The onset and autonomic regulation of cardiac pacemaker activity: relevance of the f current. *Cardiovasc. Res.* 29, 449–456.
- DiFrancesco, D., and Tortora, P. (1991). Direct activation of cardiac pacemaker channels by intracellular cyclic AMP. *Nature* 351, 145–147.
- Estevez, R., Bottger, T., Stein, V., Birkenhager, R., Otto, E., Hildebrandt, F., and Jentsch, T.J. (2001). Barttin is a Cl<sup>−</sup> channel beta-subunit crucial for renal Cl<sup>−</sup> reabsorption and inner ear K<sup>+</sup> secretion. *Nature* 414, 558–561.
- Fakler, B., Brändle, U., Glowatzki, E., Weidemann, S., Zenner, H.P., and Ruppersberg, J.P. (1995). Strong voltage-dependent inward rectification of inward rectifier K<sup>+</sup> channels is caused by intracellular spermine. *Cell* 80, 149–154.
- Feigenbaum, P., Garcia, M.L., and Kaczorowski, G.J. (1988). Evidence for distinct sites coupled to high-affinity omega-conotoxin receptors in rat-brain synaptic plasma-membrane vesicles. *Biochem. Biophys. Res. Commun.* 154, 298–305.
- Fleischmann, B.K., Duan, Y.Q., Fan, Y., Schoneberg, T., Ehlich, A., Lenka, N., Viatchenko-Karpinski, S., Pott, L., Hescheler, J., and Fakler, B. (2004). Differential subunit composition of the G protein-activated inward-rectifier potassium channel during cardiac development. *J. Clin. Invest.* 114, 994–1001.
- Garcia-Calvo, M., Knaus, H.G., Mcmanus, O.B., Giangiacomo, K.M., Kaczorowski, G.J., and Garcia, M.L. (1994). Purification and reconstitution of the high-conductance, calcium-activated potassium channel from tracheal smooth-muscle. *J. Biol. Chem.* 269, 676–682.
- Hardel, N., Harmel, N., Zolles, G., Fakler, B., and Klöcker, N. (2008). Recycling endosomes supply cardiac pacemaker channels for regulated surface expression. *Cardiovasc. Res.* 79, 52–60.
- Huang, J., Huang, A., Zhang, Q., Lin, Y.C., and Yu, H.G. (2008). Novel mechanism for suppression of hyperpolarization-activated cyclic nucleotide-gated pacemaker channels by receptor-like tyrosine phosphatase- $\alpha$ . *J. Biol. Chem.* 283, 29912–29919.
- Ishii, T.M., Takano, M., Xie, L.H., Noma, A., and Ohmori, H. (1999). Molecular characterization of the hyperpolarization-activated cation channel in rabbit heart sinoatrial node. *J. Biol. Chem.* 274, 12835–12839.
- Isom, L.L., Dejongh, K.S., Patton, D.E., Reber, B.F.X., Offord, J., Charbonneau, H., Walsh, K., Goldin, A.L., and Catterall, W.A. (1992). Primary structure and functional expression of the beta-1-subunit of the rat brain sodium channel. *Science* 256, 839–842.
- Ji, G.J., Fleischmann, B.K., Bloch, W., Feelisch, M., Andressen, C., Addicks, K., and Hescheler, J. (1999). Regulation of the L-type Ca<sup>2+</sup> channel during cardiomyogenesis: switch from NO to adenylyl cyclase-mediated inhibition. *FASEB J.* 13, 313–324.
- Knaus, H.G., Koch, R.O.A., Eberhart, A., Kaczorowski, G.J., Garcia, M.L., and Slaughter, R.S. (1995). [I-125] Margatoxin, an extraordinarily high-affinity ligand for voltage-gated potassium channels in mammalian brain. *Biochemistry* 34, 13627–13634.
- Kuise, M., Wanaverbecq, N., Brewster, A.L., Freere, S.G.A., Pinault, D., Baram, T.Z., and Luthi, A. (2006). Functional stabilization of weakened thalamic pacemaker channel regulation in rat absence epilepsy. *J. Physiol.* 575, 83–100.
- Lammel, S., Hetzel, A., Häckel, O., Jones, I., Liss, B., and Roeper, J. (2008). Unique properties of mesoprefrontal neurons within a dual mesocorticolimbic dopamine system. *Neuron* 57, 760–773.
- Larkman, P.M., and Kelly, J.S. (1992). Ionic mechanisms mediating 5-Hydroxytryptamine-evoked and noradrenaline-evoked depolarization of adult rat facial motoneurons. *J. Physiol.* 456, 473–490.
- Li, C.H., Zhang, Q., Teng, B., Mustafa, S.J., Huang, J.Y., and Yu, H.G. (2008). Src tyrosine kinase alters gating of hyperpolarization-activated HCN4 pacemaker channel through Tyr(531). *Am. J. Physiol. Cell Physiol.* 294, C355–C362.
- Ludwig, A., Zong, X.G., Jeglitsch, M., Hofmann, F., and Biel, M. (1998). A family of hyperpolarization-activated mammalian cation channels. *Nature* 393, 587–591.
- Maccaferri, G., and McBain, C.J. (1996). The hyperpolarization-activated current (I-h) and its contribution to pacemaker activity in rat CA1 hippocampal stratum oriens-alveus interneurons. *J. Physiol.* 497, 119–130.

- Magee, J.C. (1999). Dendritic I-h normalizes temporal summation in hippocampal CA1 neurons. *Nat. Neurosci.* 2, 508–514.
- Monteggia, L.M., Eisch, A.J., Tang, M.D., Kaczmarek, L.K., and Nestler, E.J. (2000). Cloning and localization of the hyperpolarization-activated cyclic nucleotide-gated channel family in rat brain. *Brain Res. Mol. Brain Res.* 87, 129–139.
- Notomi, T., and Shigemoto, R. (2004). Immunohistochemical localization of I<sub>h</sub> channel subunits, HCN1–4, in the rat brain. *J. Comp. Neurol.* 471, 241–276.
- Pandey, A., Andersen, J.S., and Mann, M. (2000). Use of mass spectrometry to study signaling pathways. *Sci. STKE* 2000, PL1.
- Pape, H.C., and McCormick, D.A. (1989). Noradrenaline and serotonin selectively modulate thalamic burst firing by enhancing a hyperpolarization-activated cation current. *Nature* 340, 715–718.
- Pfeifer, A., Kessler, T., Yang, M., Baranov, E., Kootstra, N., Cheresch, D.A., Hoffman, R.M., and Verma, I.M. (2001). Transduction of liver cells by lentiviral vectors: Analysis in living animals by fluorescence imaging. *Mol. Ther.* 3, 319–322.
- Pfeifer, A., Ikawa, M., Dayn, Y., and Verma, I.M. (2002). Transgenesis by lentiviral vectors: lack of gene silencing in mammalian embryonic stem cells and preimplantation embryos. *Proc. Natl. Acad. Sci. USA* 99, 2140–2145.
- Pian, P., Bucchi, A., Robinson, R.B., and Siegelbaum, S.A. (2006). Regulation of gating and rundown of HCN hyperpolarization-activated channels by exogenous and endogenous PIP2. *J. Gen. Physiol.* 128, 593–604.
- Reppel, M., Sasse, P., Piekorz, R., Tang, M., Roell, W., Duan, Y.Q., Kletke, A., Hescheler, J., Nurnberg, B., and Fleischmann, B.K. (2005). S100A1 enhances the L-type Ca<sup>2+</sup> current in embryonic mouse and neonatal rat ventricular cardiomyocytes. *J. Biol. Chem.* 280, 36019–36028.
- Rettig, J., Heinemann, S.H., Wunder, F., Lorra, C., Parcej, D.N., Dolly, J.O., and Pongs, O. (1994). Inactivation properties of voltage-gated K<sup>+</sup>-channels altered by presence of beta-subunit. *Nature* 369, 289–294.
- Robinson, R.B., and Siegelbaum, S.A. (2003). Hyperpolarization-activated cation currents: from molecules to physiological function. *Annu. Rev. Physiol.* 65, 453–480.
- Sanguinetti, M.C., Curran, M.E., Zou, A., Shen, J., Spector, P.S., Atkinson, D.L., and Keating, M.T. (1996). Coassembly of K(v)LQT1 and minK (IsK) proteins to form cardiac I-Ks potassium channel. *Nature* 384, 80–83.
- Santoro, B., and Tibbs, G.R. (1999). The HCN gene family: Molecular basis of the hyperpolarization-activated pacemaker channels. *Ann. N Y Acad. Sci.* 868, 741–764.
- Santoro, B., Liu, D.T., Yao, H., Bartsch, D., Kandel, E.R., Siegelbaum, S.A., and Tibbs, G.R. (1998). Identification of a gene encoding a hyperpolarization-activated pacemaker channel of brain. *Cell* 93, 717–729.
- Santoro, B., Wainger, B.J., and Siegelbaum, S.A. (2004). Regulation of HCN channel surface expression by a novel C-terminal protein-protein interaction. *J. Neurosci.* 24, 10750–10762.
- Santoro, B., Piskrowski, R.A., Pian, P., Hu, L., Liu, H., and Siegelbaum, S.A. (2009). TRIP8b splice variants form a family of auxiliary subunits that regulate gating and trafficking of HCN channels in the brain. *Neuron* 62, this issue, 802–813.
- Schagger, H., Cramer, W.A., and Vonjagow, G. (1994). Analysis of molecular masses and oligomeric states of protein complexes by blue native electrophoresis and isolation of membrane protein complexes by 2-dimensional native electrophoresis. *Anal. Biochem.* 217, 220–230.
- Schulte, U., Thumfart, J.O., Klöcker, N., Sailer, C.A., Bildl, W., Biniossek, M., Dehn, D., Deller, T., Eble, S., Abbass, K., et al. (2006). The epilepsy-linked Lgi1 protein assembles into presynaptic Kv1 channels and inhibits inactivation by Kvbeta1. *Neuron* 49, 697–706.
- Schwenk, J., Harmel, N., Zolles, G., Bildl, W., Kulik, A., Heimrich, B., Chisaka, O., Jonas, P., Schulte, U., Fakler, B., and Klöcker, N. (2009). Functional proteomics identify cornichon proteins as auxiliary subunits of AMPA receptors. *Science* 323, 1313–1319.
- Seifert, R., Scholten, A., Gauss, R., Mincheva, A., Lichter, P., and Kaupp, U.B. (1999). Molecular characterization of a slowly gating human hyperpolarization-activated channel predominantly expressed in thalamus, heart, and testis. *Proc. Natl. Acad. Sci. USA* 96, 9391–9396.
- Stevens, D.R., Seifert, R., Bufo, B., Muller, F., Kremmer, E., Gauss, R., Meyerhof, W., Kaupp, U.B., and Lindemann, B. (2001). Hyperpolarization-activated channels HCN1 and HCN4 mediate responses to sour stimuli. *Nature* 413, 631–635.
- Stieber, J., Stockl, G., Herrmann, S., Hassfurth, B., and Hofmann, F. (2005). Functional expression of the human HCN3 channel. *J. Biol. Chem.* 280, 34635–34643.
- Surges, R., Brewster, A.L., Bender, R.A., Beck, H., Feuerstein, T.J., and Baram, T.Z. (2006). Regulated expression of HCN channels and cAMP levels shape the properties of the h current in developing rat hippocampus. *Eur. J. Neurosci.* 24, 94–104.
- Svoboda, K.R., and Lupica, C.R. (1998). Opioid inhibition of hippocampal interneurons via modulation of potassium and hyperpolarization-activated cation (I-h) currents. *J. Neurosci.* 18, 7084–7098.
- Wainger, B.J., DeGennaro, M., Santoro, B., Siegelbaum, S.A., and Tibbs, G.R. (2001). Molecular mechanism of cAMP modulation of HCN pacemaker channels. *Nature* 411, 805–810.
- Wang, J., Chen, S., and Siegelbaum, S.A. (2001). Regulation of hyperpolarization-activated HCN channel gating and cAMP modulation due to interactions of COOH terminus and core transmembrane regions. *J. Gen. Physiol.* 118, 237–250.
- Wang, M., Ramos, B.P., Paspalas, C.D., Shu, Y.S., Simen, A., Duque, A., Vijayraghavan, S., Brennan, A., Dudley, A., Nou, E., et al. (2007). alpha 2A-adrenoceptors strengthen working memory networks by inhibiting cAMP-HCN channel signaling in prefrontal cortex. *Cell* 129, 397–410.
- Williams, S.R., and Stuart, G.J. (2000). Site independence of EPSP time course is mediated by dendritic I-h in neocortical pyramidal neurons. *J. Neurophysiol.* 83, 3177–3182.
- Willoughby, D., and Cooper, D.M.F. (2007). Organization and Ca<sup>2+</sup> regulation of adenylyl cyclases in cAMP microdomains. *Physiol. Rev.* 87, 965–1010.
- Zolles, G., Klöcker, N., Wenzel, D., Weisser-Thomas, J., Fleischmann, B.K., Roeper, J., and Fakler, B. (2006). Pacemaking by HCN channels requires interaction with phosphoinositides. *Neuron* 52, 1027–1036.
- Zong, X., Eckert, C., Yuan, H., Wahl-Schott, C., Abicht, H., Fang, C., Li, R., Mistrik, P., Gerstner, A., Much, B., et al. (2005). A novel mechanism of modulation of hyperpolarization-activated cyclic nucleotide-gated channels by Src kinase. *J. Biol. Chem.* 280, 34224–34232.